X-601-69-373

PREPRINT

NASA TM X- 63673

SUMMARY OF PARTICLE POPULATIONS IN THE MAGNETOSPHERE

JAMES I. VETTE

SEPTEMBER 1969

GODDARD SPACE FLIGHT CENTER
GREENBELT, MARYLAND

X-601-69-373

SUMMARY OF PARTICLE POPULATIONS IN THE MAGNETOSPHERE*

James I. Vette
National Space Science Data Center

September 1969

GODDARD SPACE FLIGHT CENTER
Greenbelt, Maryland

*Presented at Earth's Particles and Fields 1969 Symposium, Santa Barbara, Calif. Aug. 4–15, 1969.

SUMMARY OF PARTICLE POPULATIONS IN THE MAGNETOSPHERE

James I. Vette
National Space Science Data Center

ABSTRACT

The main emphasis in this summary description is on the time averaged behavior rather than the detailed dynamical changes which occur. The magnetosphere is discussed as three separate regions: plasma sheet, pseudo-trapping and stable trapping. The plasma sheet extends across the tail of the magnetosphere and contains electrons and protons with anaaverage energy of 0.6 keV and 5 keV respectively. The average outer boundary of the pseudo-trapping region is around 12 R_E. This region is spatially coincident with the auroral zone and represents an acceleration region where electrons are increased in energy to ~100 keV. In an average radial profile, particle fluxes in this region are seen only as a continuation of the radiation belts; however the shorter term time variations seen on individual satellite passes are quite distinctive. The low altitude boundary mapped on the equatorial plane by using the average magnetic field configuration presented by Fairfield agrees well with the boundary obtained in the equatorial plane except in the dawn-midnight quadrant. This difference may lead to an explanation of the dawn-dusk electron asymmetry seen at 17-18 R_E. The stable trapping boundary exists at 8 R_E. Within this region the inner and outer electron belts are seen. The average flux values and energy spectra of outer zone electrons over the 1959-1966 time period is presented. The main change over the solar cycle seems to be a filling up of the slot region starting at the slot outer edge. This results in the slot minimum moving inward as solar maximum is approached. The inner zone electron fluxes reached natural backgrounds in 1966 for energies below 1 MeV. All higher energies are the residue of Starfish and the monotonic decay of these particles continues. Protons are relatively stable in the trapping region. The proton flux models are being updated to include new higher energy results obtained near the equator.

CONTENTS

SUMMARY OF PARTICLE POPULATIONS IN THE MAGNETOSPHERE

INTRODUCTION

The purpose of this paper is to provide a succinct description of the charged particle distributions within the magnetosphere which has been made possible by the many satellite observations over the past decade. The main emphasis will be on the time averaged behavior of these particle populations rather than the detailed dynamical charges which occur. Some of the important physical processes which produce these changes are discussed elsewhere in this volume. Furthermore, many of the papers presented later will give new data, new interpretations, and generally new understanding of this complex environment. Consequently this work does not attempt to present a complete review of the previous observational measurements but rather to provide an average baseline from which the transient events depart.

The main constituents from a particle radiation standpoint are electrons and protons. Alpha particles and heavier nuclei play a smaller but significant role in understanding the various processes. Within the magnetosphere electrons range in energy from the thermal region (eV) up to several MeV while proton energies extend from thermal values up to several hundred MeV. The lower energy particles are generally spread throughout the whole cavity although certain natural boundaries can be defined for various classes of particles. The most energetic natural electrons exist around 3 to 4 R_E; the Starfish injected electrons have decayed considerably but still dominate the inner zone for energies above 1 MeV. Energetic protons peak around 1.5 R_E.

Because the particle populations and time behavior are different in many parts of the magnetosphere, it will be convenient to dissect the cavity into three basic regions: the plasma sheet, pseudo-trapping, and stable trapping regions. The average extent of these regions near the earth's geomagnetic plane is shown in Figure 1. During disturbed conditions these boundaries can change by several earth radii. We will now proceed to characterize the fluxes in these regions and to discuss Figure 1 in more detail.

PLASMA SHEET

The inner boundary of the plasma sheet has been mapped by Vasyliunas (1968) using OGO 1 and 3 electron measurements in the .04 to 2 keV energy range. This region is identified with the soft electron band first detected by

Gringauz et al. (1960a, b). During magnetic bays the boundary of the plasma sheet on the evening side of the magnetosphere moves inward to the stable trapping boundary shown in Figure 1 and sometimes pushes in to 5.5 R_E. However, the plasma sheet has not been observed to penetrate the plasmasphere. The complete radial extent of the sheet is not presently known; it has been studied recently at lunar distances by Nishida et al. (1969) where its properties are similar to those at 18 R_E.

The plasma sheet is present at all times and extends across the tail of the magnetosphere. The sheet is 4-6 R_E thick in the center and flares out to 8 to 12 R_E in thickness toward the dawn and dusk boundaries. The most extensive spectral properties of this plasma have been measured by the Vela satellites at 17 R_E and have been summarized by Bame (1968). The electron spectrum is quasi-thermal with a high energy tail. The average electron energy is 0.6 keV but varies from 0.1 to 10 keV. Omnidirectional fluxes >100 eV extend to 10^9 cm^{-2}-sec^{-1} and the particle density ranges from 0.1 to 3 cm^{-3} with an average value of 0.5. Vasyliunas (1968) has obtained densities up to 30 cm^{-3} with a lower energy threshold. The energy density of the protons in the plasma sheet exceeds that of electrons by a factor of about 8. The average proton energy is 5 keV and ranges from 1 to 20 keV. Of course, the plasma is neutral so electron and proton densities are the same.

The high energy tail of both these particle distributions have been detected by many different instruments. A radial profile has been obtained using detectors sensitive to electrons > 30 to 45 keV with an intensity limit of 10^4 cm^{-2}-sec^{-1} (Anderson, 1965; Murayama, 1966). With these instruments there are many times when no fluxes are observed past ~7 R_E. When they are observed, the events are called islands which exhibit fluxes up to 10^7 cm^{-2}-sec^{-1}, which are nearly as intense as those found in the radiation belts. The majority of these events show a fast rise time and a slow decay leading to the suggestion by Anderson that these variations are temporal and not spatial. Murayama has shown the frequency of these events are independent of radial distance (between 15 to 31 R_E) but are strongly correlated with the distance from the magnetic neutral sheet and are confined within the thickness of the plasma sheet. The frequency of events increases with magnetic activity. Konradi (1966) has reported proton islands with intensities ~10^5 cm^{-2}-sec^{-1} and energies >125 keV. The integral proton energy spectrum can be approximated by a power law with an exponent lying between 5 to 8. Both the high intensity proton and electron island events probably represent an energization within the plasma sheet. Recently Retzler and Simpson (1969) have reported observations of 400 keV electron island events in the plasma sheet. Detailed observations by Montgomery (1968) provide a good picture at 17 to 18 R_E. The frequency of occurrence of electron fluxes >64 keV is shown as a function of solar magnetospheric coordinates in Figure 2. The dawn-dusk asymmetry can clearly be seen (Figure 1).

The integral energy spectrum of these electrons can be approximated by a power law with an average exponent ranging between 3 and 4 which shows no systematic change with solar magnetospheric longitude. The extreme excursions of this exponent vary from 1 to 7.

The inner boundary of the plasma sheet has not been reported yet in the midnight-dawn quadrant. We have made a distinction in Figure 1 between the normal plasma sheet and the region where Montgomery nearly always detects a high energy electron tail.

PSEUDO-TRAPPING REGION

This region has been referred to as the distant radiation zone by Anderson (1965). It was recognized that particles in this region could not execute complete drift motion around the earth but could exhibit complete bounce and partial drift motion. The skirt (Figure 1) was first described by Frank et al. (1963) and was subsequently discussed by Anderson et al. (1965) and Frank (1965). The cusp, which is confined to low latitudes $\sim \pm 20^{\circ}$, was also detected by these investigators. Roederer (1967) calculated the adiabatic motion of particles using the Mead-Williams model (Mead, 1964; Williams and Mead, 1965) and the geometric extent of the pseudo-trapping regions agreed reasonably well with the experimental results for the skirt and the cusp. The outer edge of the pseudo-trapping region shown in Figure 1 was determined by ~40 to 100 keV electrons at low latitudes from results on Explorer 14 by Frank (1965), Explorer 21 (IMP 2) by Rothwell and Lyman (1969) and ERS-17 by Vette (Peterson et al. 1968). The various particle boundaries also can be detected at high latitude by low altitude satellites. McDiarmid and Burrows (1968) have presented results from Alouette 1 and 2. The various boundaries are shown in Figure 3 along with Feldstein's (1966) auroral oval and the 280 keV boundary given by Williams and Mead (1965). We have projected the Alouette 2 stable trapping boundary and the outer limit of trapping onto the equatorial plane using the average magnetic field configuration given by Fairfield (1968). The stable trapping boundary is shown in Figure 1 as the high energy electron region and is in essential agreement with the low latitude 1.6 MeV electron boundary obtained on IMP 2 by Rothwell and Lyman (1969). On the dusk side of the earth from 1200 to 2400 LT, the Alouette outer trapping boundary follows the low latitude boundary given in Figure 1. However on the dawn side the high latitude boundary maps into the magnetopause over the 1200 to 0600 hr. local time interval. For local times between 0200 to 0600 hr., the boundary extends out in the equatorial plane to large distances. These results, along with those of Montgomery (1968), suggest that the clear region shown in Figure 1 is a special one in the magnetosphere bearing further investigation.

The close spatial relationship between the auroral zone and the pseudo-trapping region can readily be seen in Figure 3. Kennel (1969) has recently

reviewed the electron and proton discontinuities in the auroral zone. He has made the following conclusions on the basis of experimental evidence:

1. Soft electrons from the plasma sheet have a sharp inner boundary which corresponds with a sharp outer boundary of harder Van Allen belt electrons;

2. The auroral electron discontinuity is continuously present but moves in response to geomagnetic activity. During substorms the discontinuity moves closer to the earth;

3. Electrons up to ~100 keV approach pitch angle isotropy at the discontinuity both inside and near the loss cone suggesting a strong diffusion mechanism;

4. Electrons are locally accelerated to energies of a few hundred keV at the discontinuity and precipitated particles maximize in this region where isotropy of fluxes are approached; and

5. A similar proton boundary lies closer to the earth and often coincides with the plasmapause. Precipitating protons also tend toward isotropy.

Recently, Chase (1969) has shown that the flux and spectrum of precipitating electrons in the auroral zone on occasion has the same flux and spectrum as that for electrons in the plasma sheet suggesting that the plasma sheet is the source of these particles.

Frank (1967, 1968) has presented some results of protons and electrons in this region of the magnetosphere convering the energy range ~200 eV to 50 keV in 13 energy bands. These OGO 3 measurements show a rich and varied behavior which are difficult to summarize. Some of Frank's proton results for one pass through the cusp region are shown in Figure 4 in order to present some representative flux values. Electron results on a similar pass are given in Figure 5. The detailed analysis of this experiment will provide a much greater understanding of the pseudo-trapping region and will permit average flux values to be obtained in this energy range. Average electron flux values above 40 keV in this spatial region are presented later in Figures 7 and 8. The sharp boundaries which appear on individual satellite passes to distinguish the pseudo-trapping region are not seen in the time averaged radial profile. The pseudo-trapping region seems to be a thick transition layer between the plasma sheet and the Van Allen radiation belt where particles are accelerated to higher energy. Obviously other accelerations must occur within the stable trapping region in order to account for the even higher energy particles found in the inner and outer radiation zones.

STABLE TRAPPING REGION

The extent of the stable trapping region is shown in Figure 1 where the 65 γ B contour of Fairfield has been used to limit the region on the sunward side. Some of the particles which mirror at high latitude and pass through this region in the equatorial plane are pseudo-trapped so that the omnidirectional equatorial flux is composed of both types of particles. However, within the high energy electron boundary all of the particles will normally be trapped. During magnetic storms and substorms the magnetospheric cavity undergoes dramatic changes; particles within the cavity are both adiabatically and non-adiabatically accelerated. The boundaries shown in Figure 1 shift inward by several earth radii and very likely new particles accelerated from the plasma sheet in the pseudo-trapping region are fed into the stable trapping region. The main consequence of these complicated events is that the electron and proton fluxes show rather sharp increases or decreases depending on the particle energy, the particular event, and the position. Protons show less change than electrons both in frequency of occurrence and in magnitude. The details of particular storm changes have been discussed by numerous authors.

In view of the one to two order of magnitude change of electrons during these events, it is useful to determine the average value of the flux in order to obtain a background picture. Because of the distortion of the geomagnetic cavity and the existence of a tail field, the adiabatic motion of the particles is altered from that in a dipole field. Diurnal variations of the fluxes are evident past 5 R_E but it is difficult to establish the local time behavior with precision using elliptical satellite data. Fortunately the synchronous satellites provide a platform where these variations can be studied in an important region. Vette and Lucero (1967) showed that fluxes could be approximately represented by a log normal distribution in the outer zone. These results had been based on a small number of points at various $\underline{L}$ values. We show the recent results of Paulikas and Blake (1969) obtained on ATS 1 in Figure 6 compared to the AE 3 model electron environment constructed earlier by Vette and Lucero. For energies below 1 MeV the agreement is excellent except at high flux values. For all energies the log normal distribution with proper parameters seems to be a reasonable description of this data.

The average electron flux near the equator for a selected series of satellite measurements covering the time period August 1959 to March 1968 is shown in Figures 7 and 8 as a function of radial distance. Directional data have been converted to omnidirectional fluxes to facilitate comparison with the other data. The variability of the fluxes about their mean values can be expressed in terms of the standard deviation of the logarithm of the flux. This parameter is shown in Figure 9 as a function of $\underline{L}$ for some of the various measurements we have

processed. The lower energy particles show a maximum variation at L values corresponding to the pseudo-trapping region whereas the higher energy particles show a peak variation between 6 and 7 R_E. The position of the outer zone flux maximum and slot minimum as a function of the solar cycle has been presented by Vernov et al. (1969) and the slot minimum by Frank and Van Allen (1966). It should be pointed out that these parameters are really energy dependent and the position of intensity maximum can vary by 1 R_E in a few weeks. The B/Bo variation of some of the outer zone electron data is shown in Figure 10.

While the lifetime of protons in the inner zone is many years, the effective lifetime of electrons is much less than this. The electrons injected by Starfish have been decaying approximately exponentially with time. Walt (1966) has compiled the electron lifetimes obtained by various experiments which show a broad peak of 300 to 400 days between L = 1.25 and 1.7. There is rapid decline at lower L values caused by the increasing density of the earth's atmosphere; above L = 2.0 lifetimes drop abruptly to just a few days.

Recently, Bostrom et al. (1968) have presented the time behavior of trapped particles in the inner zone from October 1963 through December 1967. Electrons >1.2 MeV have decayed monotonically since the Starfish detonation. For electrons >280 keV the general vehavior has been one of exponential decay but there were definite increases during the large magnetic storms in September 1966 and May 1967. Pfitzer and Winckler (1968) have observed these same increases for electrons less than 690 keV.

Based on these latest observations, it appears that large magnetic storms can produce electrons in the inner zone with energies not exceeding about 1 MeV. Thus, all higher energy electrons present are the residue of Starfish. Between 1963 and 1966 Starfish electrons dominated the whole inner zone. By mid 1966, however, electrons below 1 MeV had decayed to the point where natural effects became apparent. For higher energies the electrons continue to decay.

High energy protons have exhibited great stability in the radiation belts. We show the 40 to 110 MeV results of McIlwain (1963; 1969) in Figure 11 for two different epochs. The second bump around L = 2.2 had begun to diffuse inward by 1965 and has probably disappeared by the present time. The results of Bostrom et al. (1968) at 1100 km showed protons above 8 MeV to be quite stable until the May 1967 event when decreases were seen for L values above 2.6. The 2 MeV protons showed a slight decay over this same time period with both increases and decreased depending on L value seen in the fluxes during the May event. Soraas and Davis (1968) have discussed the increases in protons below 180 keV and decreases for those above 345 keV in connection with the April 1965 magnetic storm. They showed that only part of the changes were adiabatic. At low

altitudes the solar cycle effect predicted by Blanchard and Hess (1964) finally has become evident. Nakano and Heckman (1968) have reported the 63 MeV protons with minimum altitudes between 220 and 375 km decreased a factor of 2 between mid 1966 and late 1967 after remaining constant for the previous 3-1/2 yr. Measurements of energetic protons with energies above 55, 105, and 170 have recently been presented by Thede (1969) which show that previous estimates near the equator in this range were low by about a factor of 3.

We show in Figure 12 a radial profile of the omnidirectional proton flux at the equator which incorporates the new high energy data of Thede. Although there are some time variations in the low energy protons, insufficient information has been presented to determine any long term trends near the equator and average values are not yet available. Therefore, at the present time, the static proton models of Vette and co-workers (Vette, 1966; king, 1967; Lavine and Vette, 1969) are all that are justified by the available data.

Finally, we cite that α-particles have been detected in the stable trapping region by Krimigis and Van Allen (1967) with the peak intensity occurring at $\underline{L} = 3.1\ R_E$. This peak was enhanced and shifted inward by $0.2\ R_E$ following the April 17, 1965 storm. Trapped α-particle measurements have also been reported by Paulikas and co-workers (Paulikas et al., 1968; Paulikas and Blake, 1968) who have obtained a power law spectrum over the range 2.8 to 6.2 MeV. The alpha to proton ratio at 0.5 MeV/nucleon varies from 2×10^{-3} to 10^{-4} as $\underline{L}$ increases from 2.2 to 4.2.

REFERENCES

Anderson, K. A.: 1965, J. Geophys. Res. 70, 4741.

Anderson, K. A., Harris, H. K., and Paoli, R. J.: 1965, J. Geophys. Res. 70, 1039.

Bame, S. J.: 1968, Earth's Particles and Fields (ed. by B. M. McCormac), Reinhold Publishing Corporation, New York, 373.

Blanchard, R. C. and Hess, W. N.: 1964, J. Geophys. Res. 69, 3927.

Bostrom, C. O., Beall, D. S., and Armstrong, J. C.: 1968, Paper presented at International Symposium on the Physics and the Magnetosphere.

Chase, L. M.: 1969, J. Geophys. Res. 74, 348.

Fairfield, D. H.: 1968, J. Geophys. Res. 73, 7329.

Feldstein, Y. I.: 1966, Planet. Space Sci. 14, 121.

Frank, L. A.: 1965, J. Geophys. Res. 70, 1593.

Frank, L. A.: 1968, Physics and the Magnetosphere (ed. by R. L. Carovillano, J. F. McClay, and H. R. Radowski), D. Reidel Publishing Company, Dordrecht-Holland, 271.

Frank, L. A. and Van Allen, J. A.: 1966, J. Geophys. Res. 71, 2697.

Frank, L. A., Van Allen, J. A., and MacAgno, E.: 1963, J. Geophys. Res. 68, 3543.

Gringauz, K. I., Bezrukikh, V. V., Ozerov, V. D., and Rybachinsky, R. Ye.: 1960a, Soviet Phys. Doklady 5, 361.

Gringauz, K. I., Kurt, V. G., Moroz, V. I., and Shklousky, I. S.: 1960b, Soviet Astron. AJ, 4, 680.

Kennel, C. F.: 1969, Rev. Geophys. 7, 379.

King, J. H.: 1967, NASA SP-3024 Vol. IV.

Konradi, A.: 1966, J. Geophys. Res. 71, 2317.

Krimigis, S. M. and Van Allen, J. A.: 1967, J. Geophys. Res. 72, 5779.

Lavine, J. P. and Vette, J. I.: 1969, NASA SP-3024 Vol. V.

McDiarmid, I. B. and Burrows, J. R.: 1968, Can. J. Phys. **46**, 49.

McIlwain, C. E.: 1963, Science **142**, 355.

McIlwain, C. E.: 1969, private communication.

Mead, G. D.: 1964, J. Geophys. Res. **69**, 1181.

Montgomery, M. D.: 1968, J. Geophys. Res. **73**, 871.

Murayama, T.: 1966, J. Geophys. Res. 71, 5547.

Nakano, G. H. and Heckman, H. H.: 1968, Phys. Rev. Letters **20**, 806.

Nishida, A., Lyon, E. F., and Ness, N. F.: 1969, private communication.

Paulikas, G. A. and Blake, J. B.: 1968, Paper presented at International symposium on the Physics of the Magnetosphere.

Paulikas, G. A. and Blake, J. B.: 1969, private communication.

Paulikas, G. A., Blake, J. B., and Freden, S. C.: 1968, Aerospace Corp. Report No. TR-0200(4260-20)-03.

Peterson, L. E., Matteson, J. L., Huszar, L., and Vette, J. I.: 1968, Univ of Calif., San Diego Report SP-68-7.

Pfitzer, K. A. and Winckler, J. R.: 1968, J. Geophys. Res. **73**, 5792.

Retzler, J. and Simpson, J. A.: 1969, J. Geophys. Res. **74**, 2149.

Roederer, J. G.: 1967, J. Geophys. Res. **72**, 981.

Rothwell, P. and Lyman, C.: 1969, Planet. Space Sci. **17**, 447.

Soraas, F. and Davis, L. R.: 1968, NASA-GSFC X-612-68-328.

Thede, A. L.: 1969, Air Force Weapons Lab. Report AFWL-TR-128.

Vasyliunas, V. M.: 1968, J. Geophys. Res. **73**, 2839.

Vette, J. I.: 1966, NASA SP-3024 Vol. I.

Vette, J. I. and Lucero, A. B.: 1967, NASA SP-3024 Vol. III.

Walt, M.: 1966, Radiation Trapped in the Earth's Magnetic Field (ed. by B. M. McCormac), D. Reidel, Dordrecht-Holland, 337.

Williams, D. J. and Mead, G. D.: 1965, J. Geophys. Res. 70, 3017.

Vernov, S. N., Gorchakov, E. V., Kuznetsov, S. N., Logachev, Y. I., Sosnovets, E. N., and Stolpuvsky, V. G.: 1969, Rev. Geophys. 7, 257.

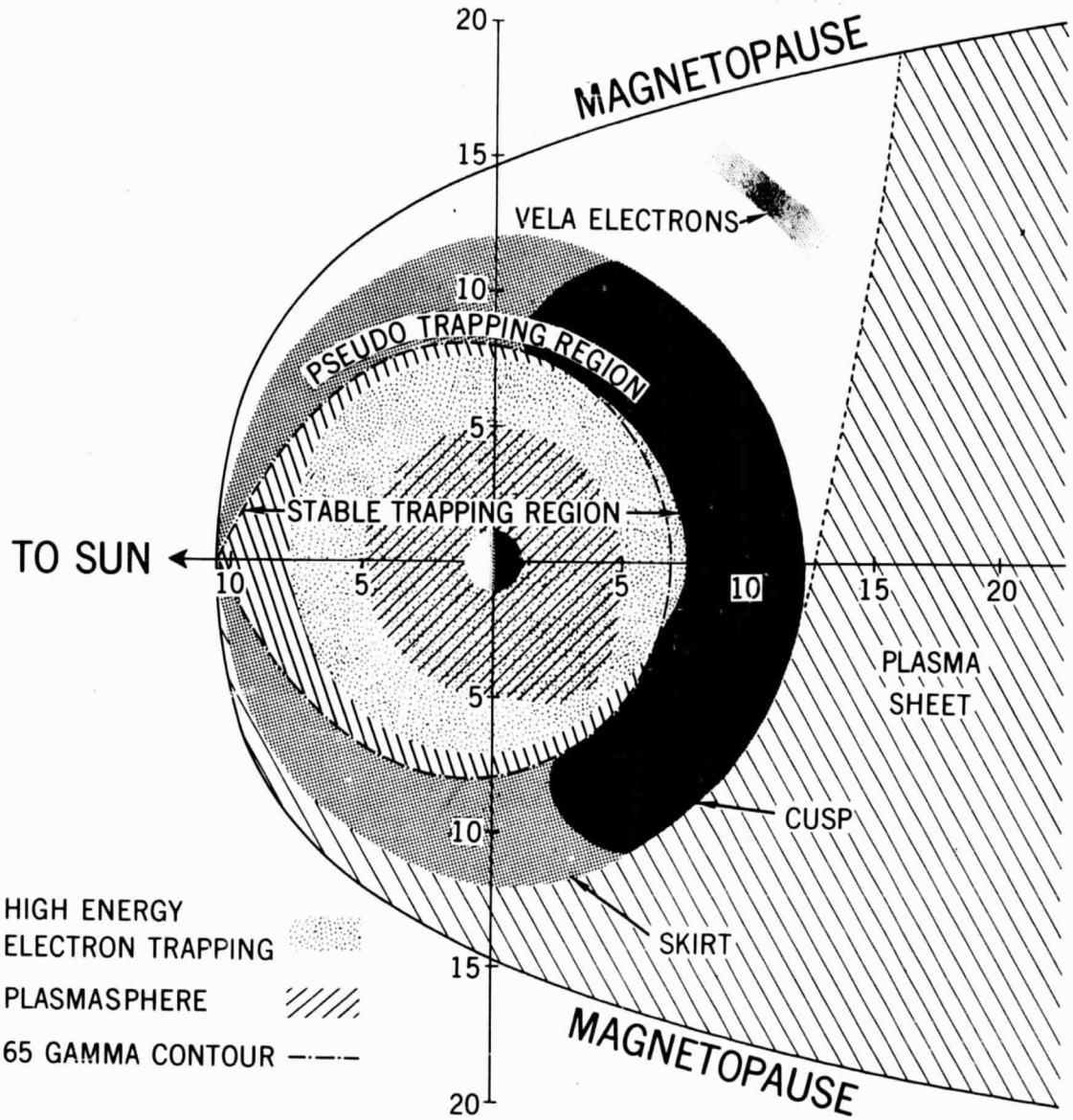

Figure 1. Regions of the magnetosphere in the equatorial plane. The regions are depicted when magnetic activity is not very high. The 65 gamma contour and the magnetopause are taken from Fairfield (1968). The dotted inner boundary of the plasma sheet in the dawn-midnight quadrant indicates this boundary has not been detected yet in this region of space.

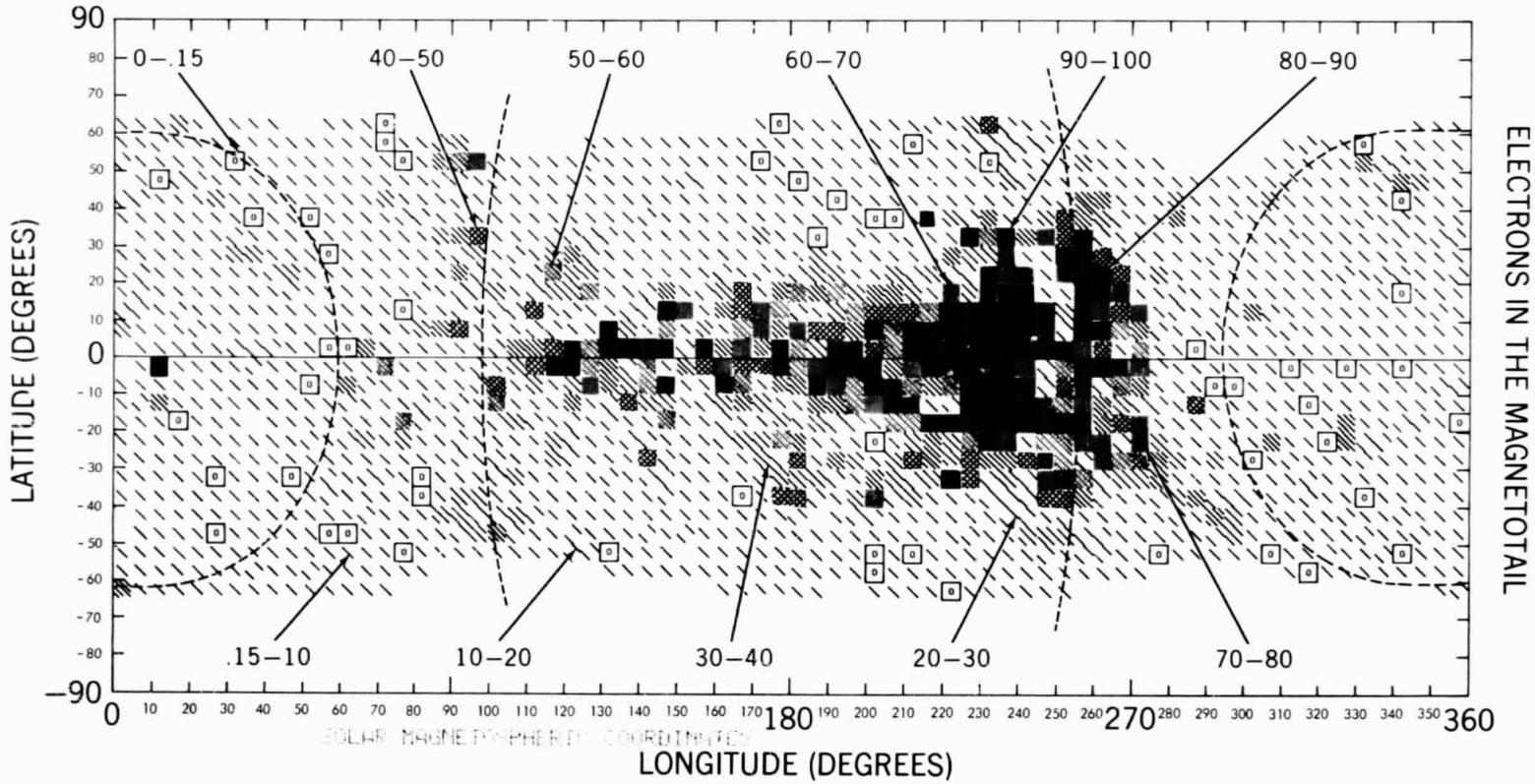

Figure 2. Frequency of occurrence of >64 keV electron fluxes in the magnetotail. The various shaded blocks represent the frequency of occurrence of fluxes greater than 83 cm^{-2}-sec^{-1}-sr^{-1} in percent for the 5° x 5° solar magnetospheric angular areas. The outer dotted lines represent the average position for the standing shock wave and the inner dotted lines represent the average position of the magnetosphere at 17 R_E (after Montgomery, 1968).

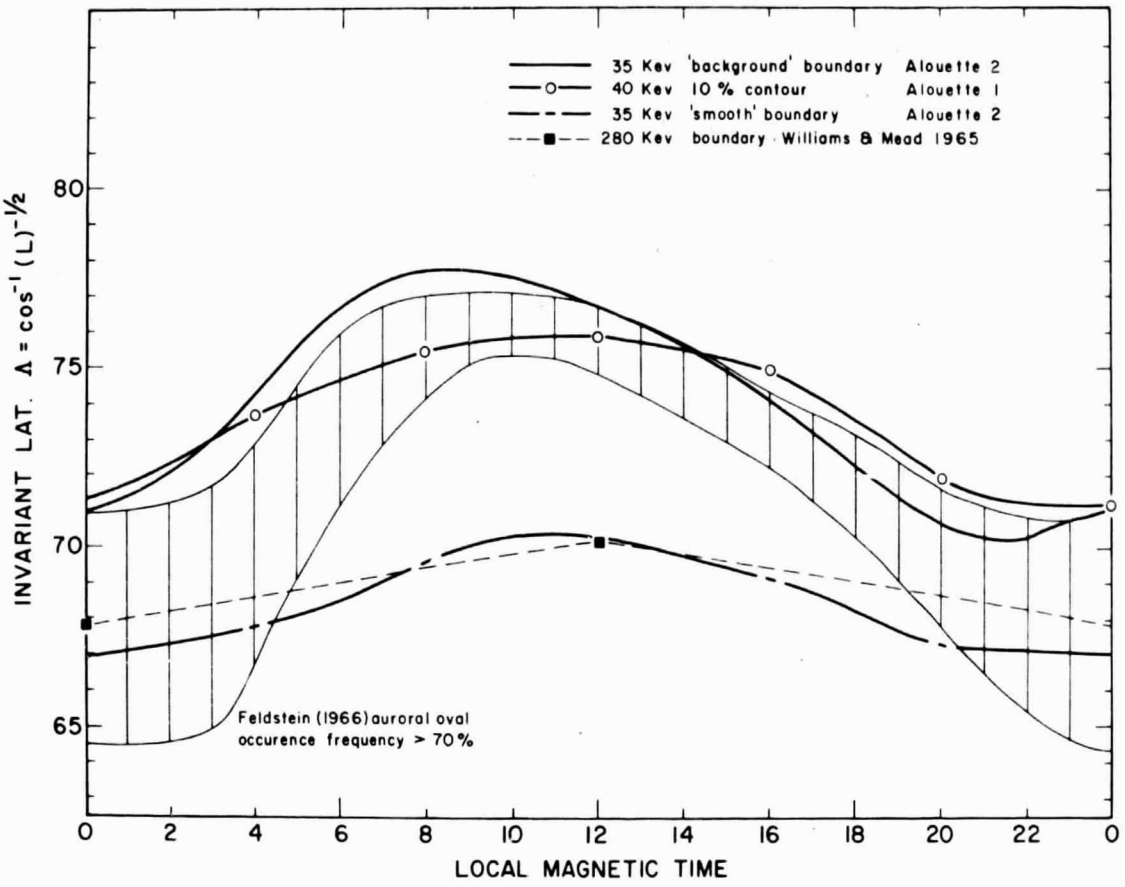

Figure 3. Comparison of various high latitude boundaries for energetic particle fluxes observed by Alouette 1 and 2 with Feldstein's auroral oval and the trapping boundary of Williams and Mead (after McDiarmid and Burrows, 1968).

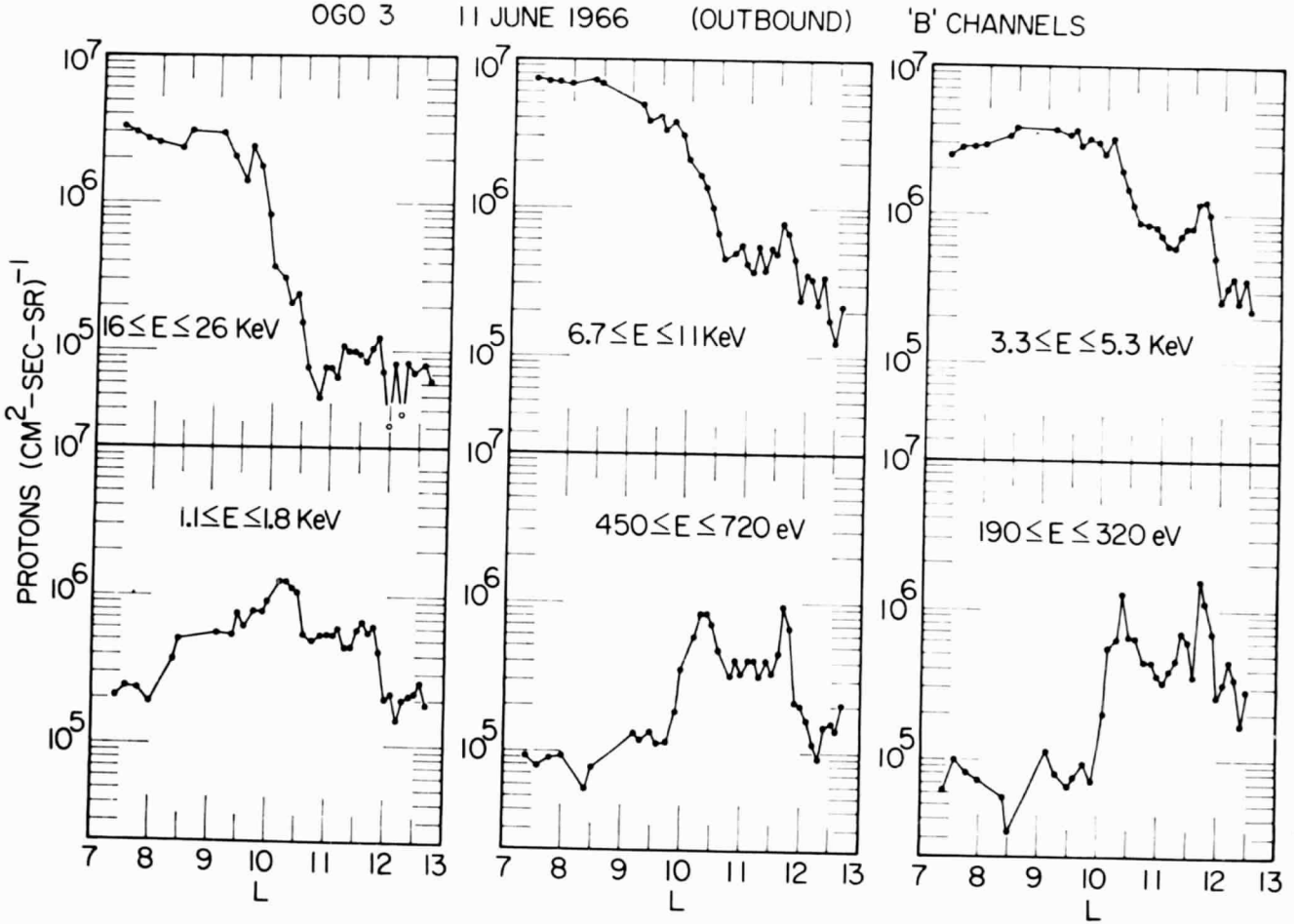

Figure 4. Directional intensity of protons observed on July 11, 1966. The solar ecliptic longitude varies from 95° at $\underline{L}$ = 7 R_E to 117° at $\underline{L}$ = 13 R_E; magnetic latitude lies between 22° and 27° (after Frank, 1967).

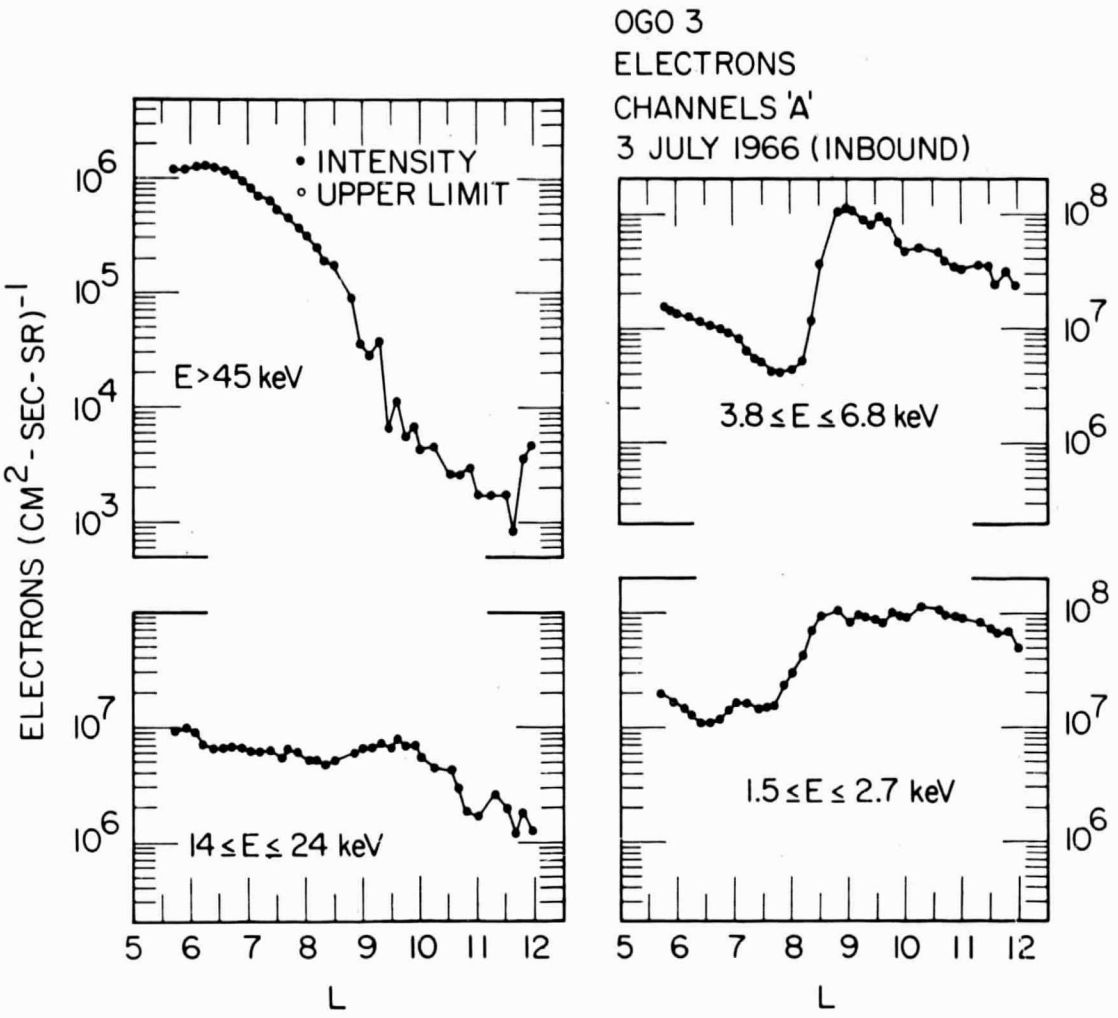

Figure 5. Directional intensity of electrons observed near the midnight meridian on June 22-23, 1966. The magnetic latitude was less than 20° for the whole period shown (after Frank, 1968).

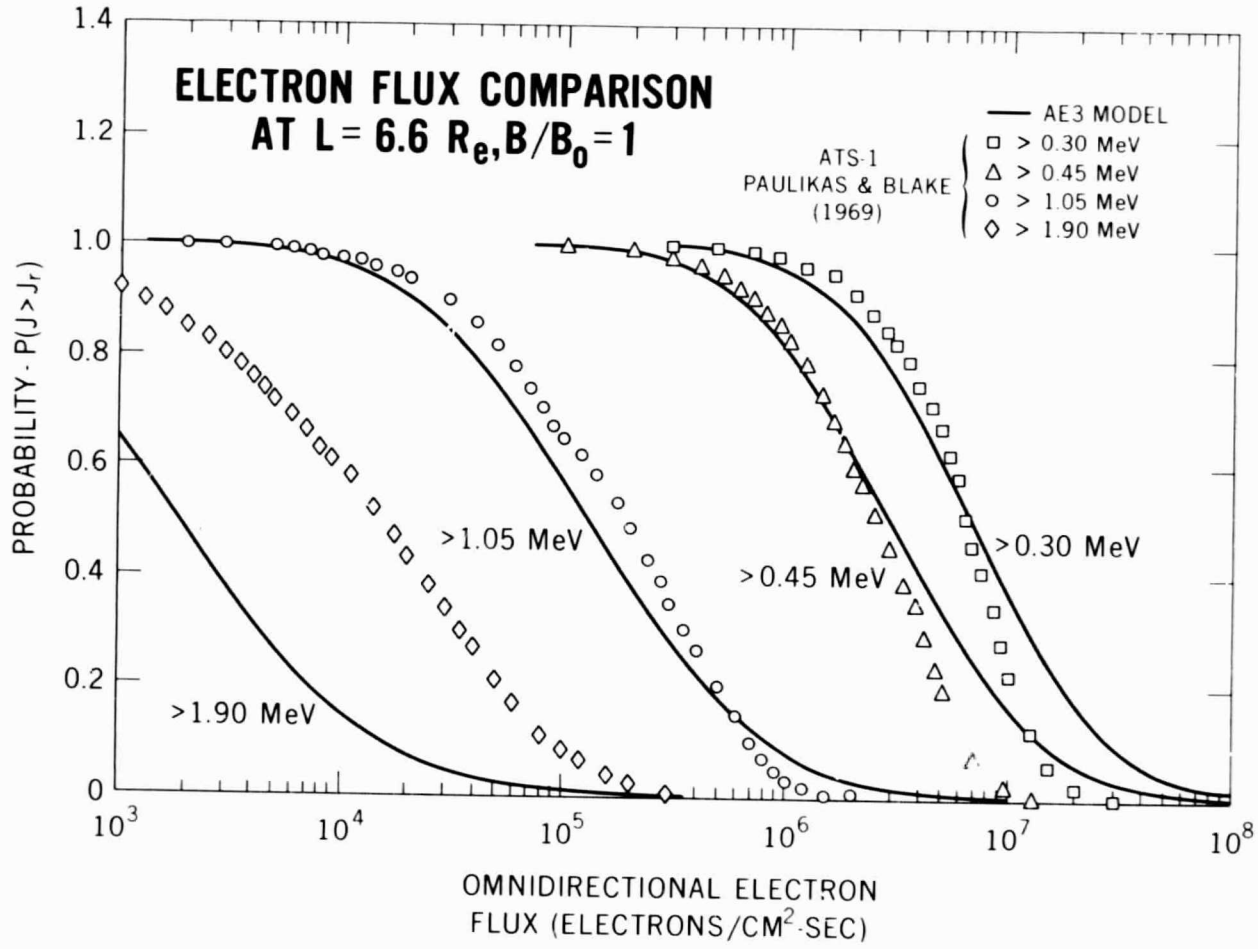

Figure 6. Comparison of ATS 1 electron fluxes with the electron model environment AE 3. The ATS results represent an average from Dec. 6, 1966 - Mar. 1, 1968 (Paulikas and Blake, 1969) while AE 3 was based on data prior to Jan. 1966.

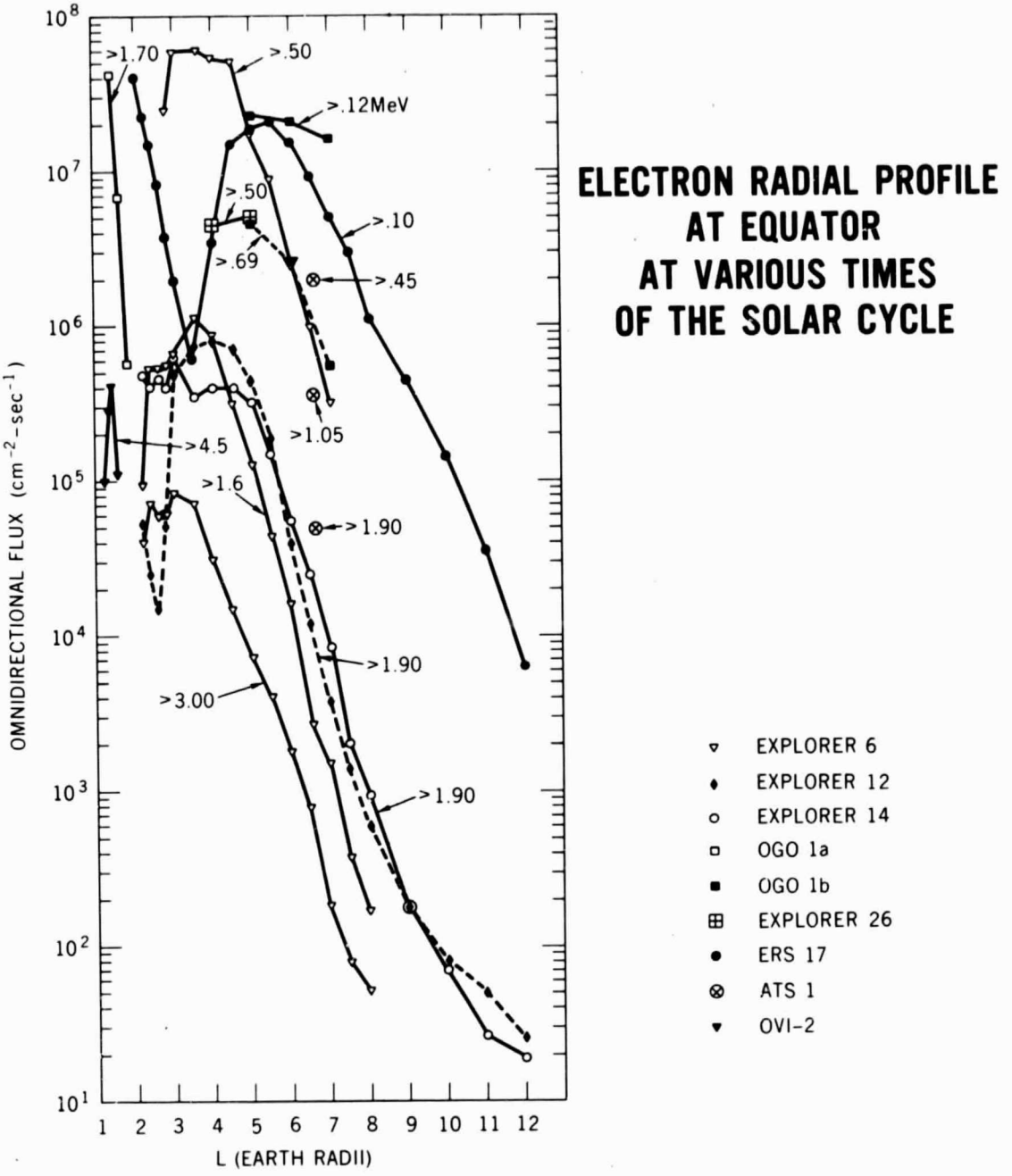

Figure 7. Time averaged omnidirectional electron fluxes at the equator. The results for $\underline{L} > 2.2$ R_E are average values obtained over the following time periods: Explorer 14 (Oct. 4, 1962 - Aug. 5, 1963); IMP 1 (Nov. 27, 1963 - May 27, 1964); OGO 1b (Sept. 21, 1964 - June 20, 1965); Explorer 26 (Dec. 21, 1964 - Aug. 10, 1965); ERS-17 (July 20, 1965 - November 3, 1965); ATS 1 (Dec. 6, 1966 - Mar. 1, 1968). The inner zone results are for the following time periods: OGO 1a (Sept. 1964 - Mar. 1965); OV1 2 (Oct. 1965).

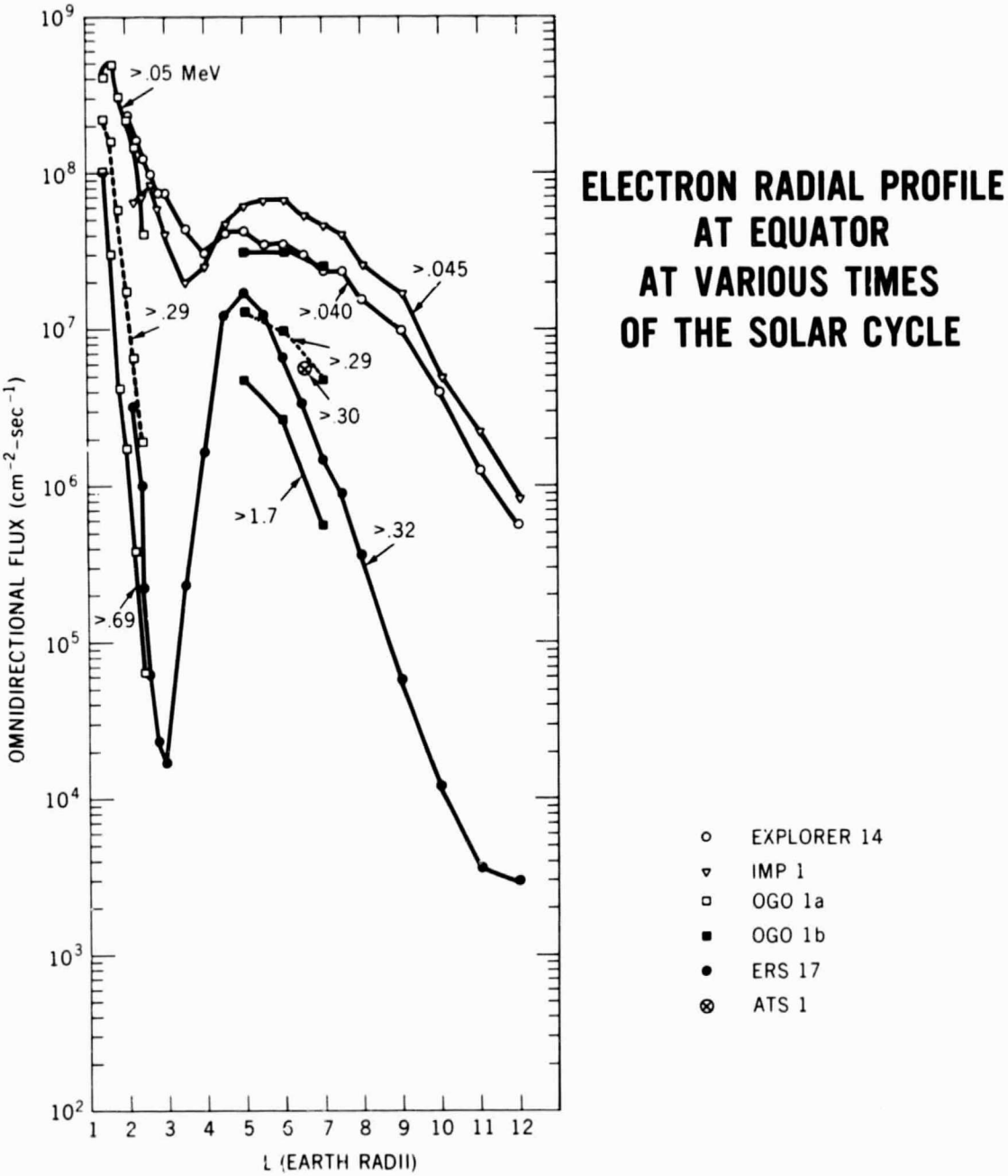

Figure 8. Time averaged omnidirectional electron fluxes at the equator. The results for $L > 2.2$ R_E are average values obtained over the following time periods: Explorer 6 (Aug. 7, 1969 - Sept. 10, 1959); Explorer 12 (Aug. 17, 1961 - Dec. 5, 1961); all other satellites the same interval as in Figure 7.

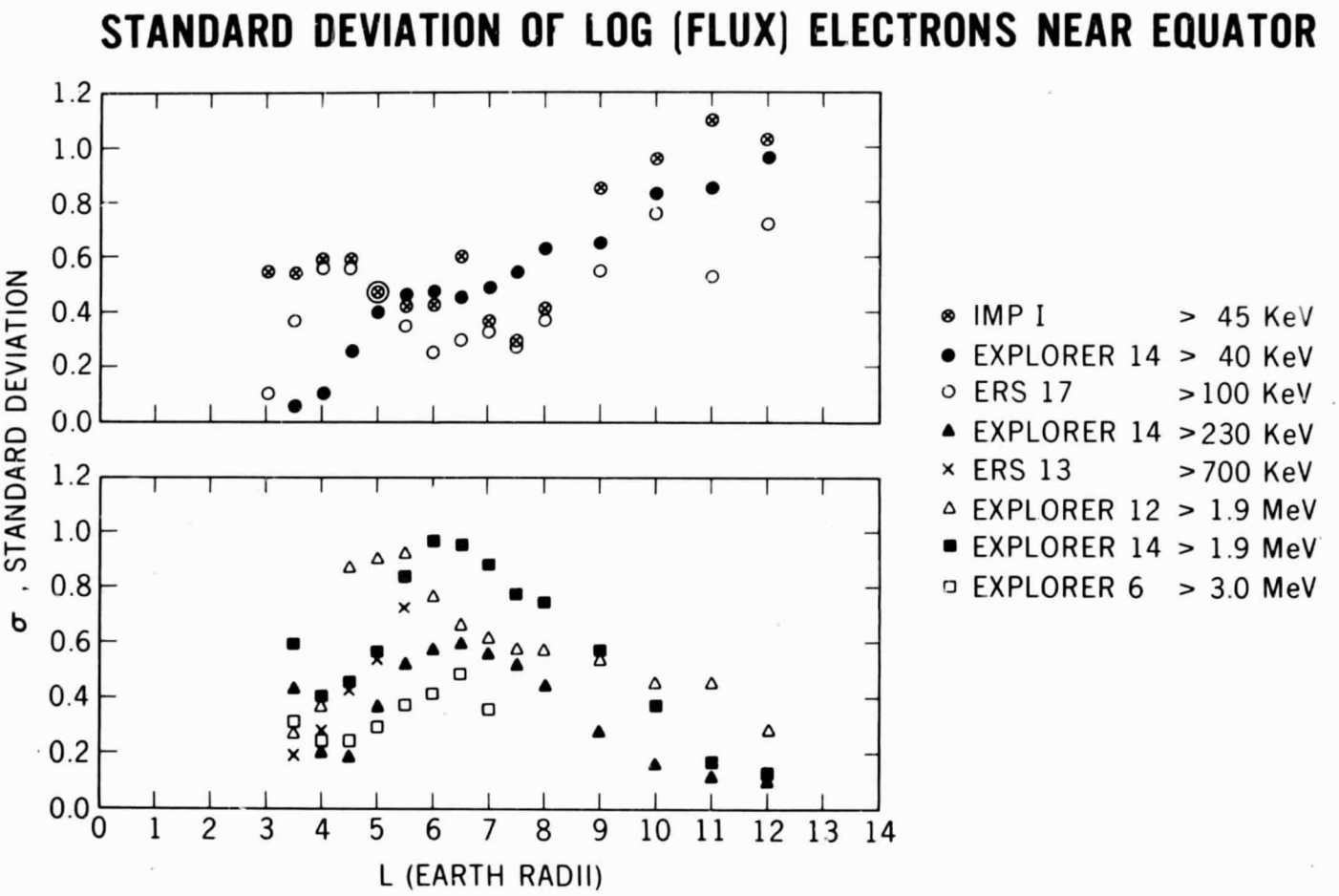

Figure 9. L variation of the standard deviation of the logarithm of the electron flux. The upper data sets are for energies below 100 keV and the lower sets are for higher energies. Notice the lower energy particles exhibit maximum variability in the pseudo-trapping region while the higher energy ones show a peak around 6 to 7 R_E.

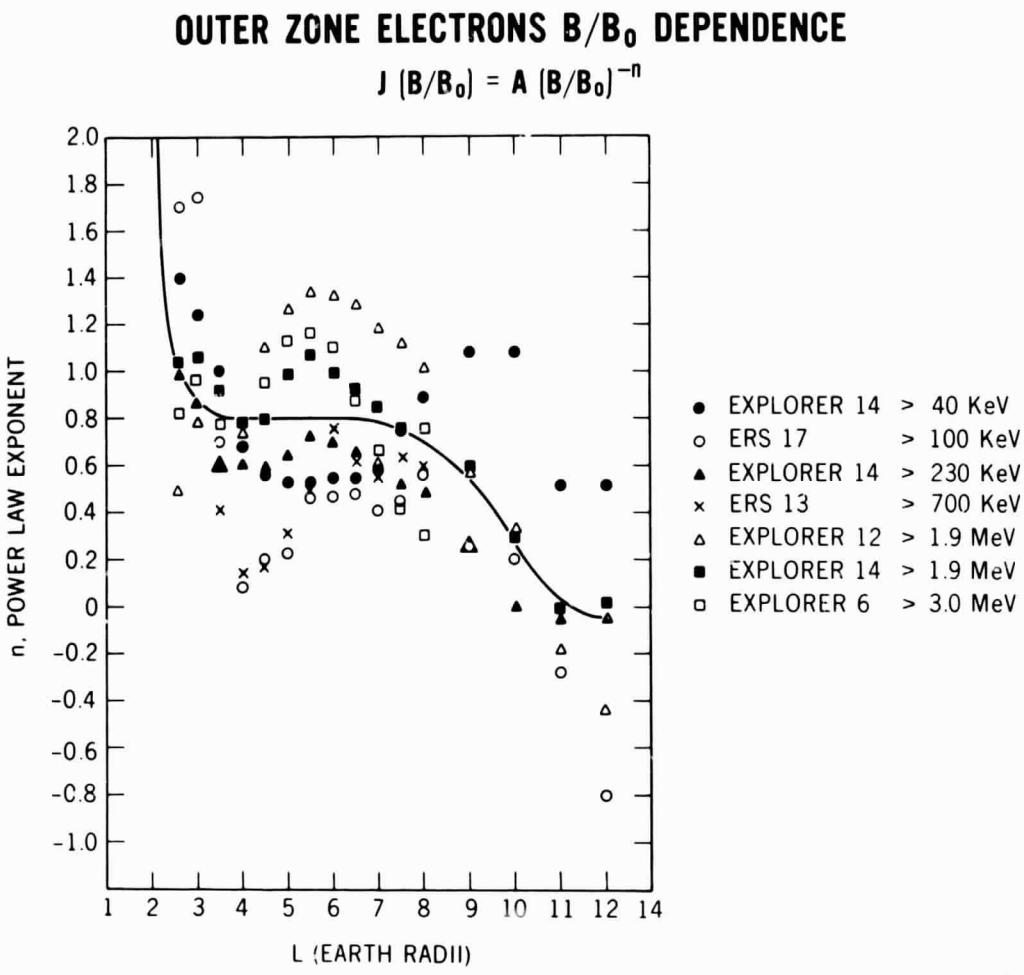

Figure 10. B/Bo variation of outer zone average electron fluxes. These data are averaged over time periods given in Figures 7 and 8. The solid line is used to provide a guide for the eye. There seems to be no systematic trend with energy except possibly in the range $4 \leq L \leq 7\ R_E$.

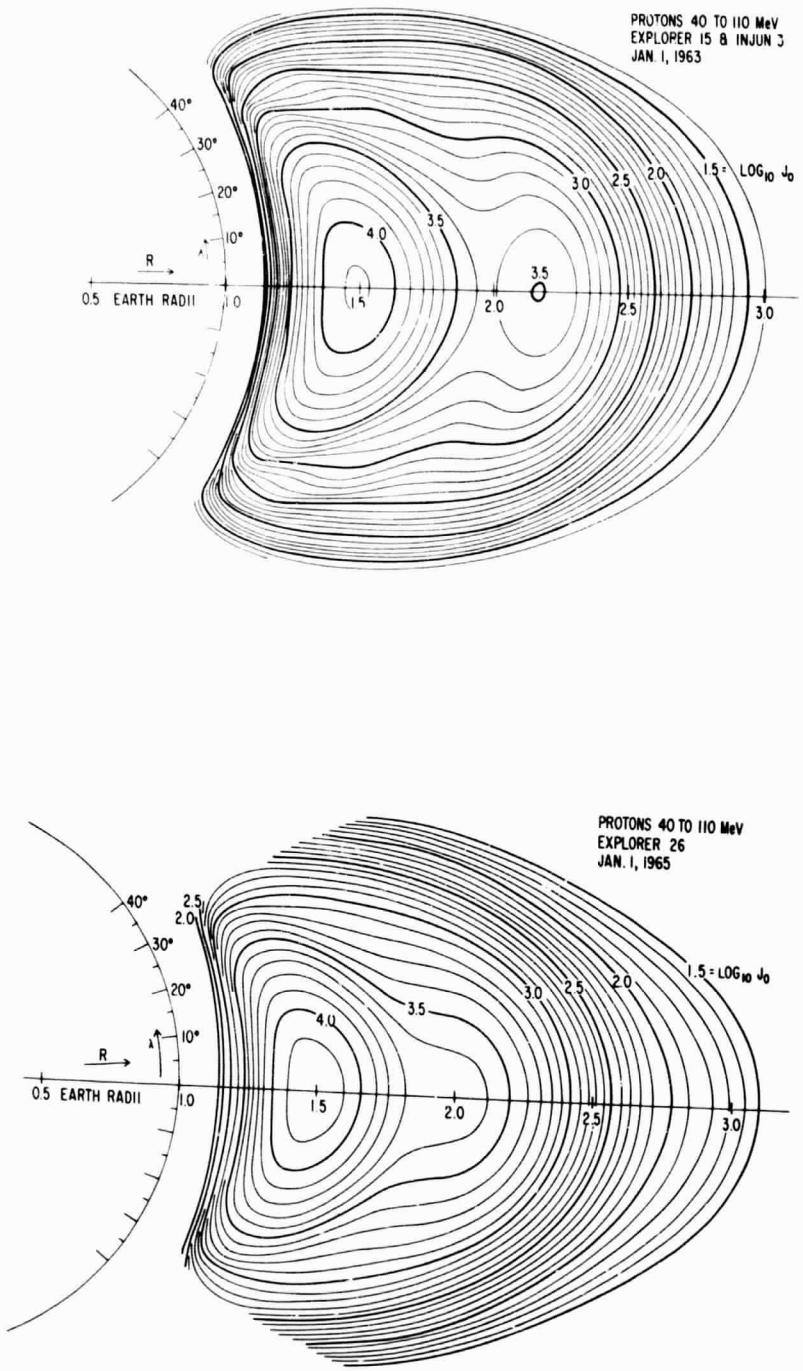

Figure 11. Comparison of 40-110 MeV protons at two different epochs. The results were obtained on Explorer 15 (McIlwain, 1963) and Explorer 26 (McIlwain, 1969).

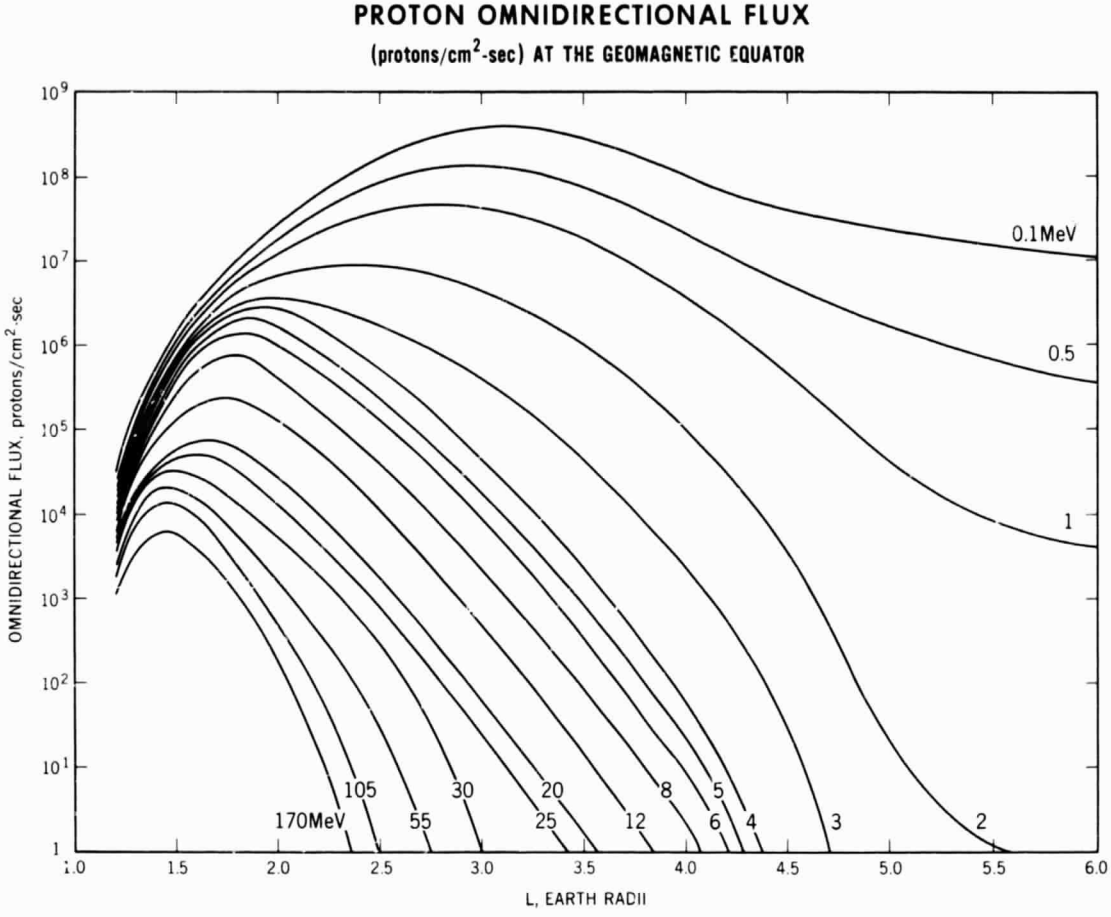

Figure 12. Radial profile of integral energy omnidirectional proton fluxes at the geomagnetic equator.